Electronic Supplementary Information

NIR-emitting squaraine J-aggregate nanosheets

Chia-An Shen[1] and Frank Würthner[1,2]*

1. Institut für Organische Chemie, Universität Würzburg, Am Hubland, 97074 Würzburg, Germany.

2. Center for Nanosystems Chemistry (CNC), Universität Würzburg, Theodor-Boveri-Weg, 97074 Würzburg, Germany.

*Email: wuerthner@uni-wuerzburg.de

Table of Contents

1. Materials and methods

General

All solvents and reagents were purchased from commercial sources and used as received without further purification. Column chromatography was performed using silica gel 60M (0.04 – 0.063 mm).

Gel permeation chromatography (GPC)

For the GPC purification method, the preparative recycling-GPC LaboACE from Japan Analytical Industry Co., Ltd. (JAI) with PLgel Prep columns (from Agilent Technologies) were used.

NMR spectroscopy

NMR spectra were recorded on a Bruker Avance 400 or Bruker Avance DMX 600 at 295 K. The spectra were calibrated to the residual solvent peak and the chemical shifts δ are given in ppm. Multiplicities are denoted as follows: s = singlet, d = doublet, t = triplet, q = quartet, quint = quintet, dd = doublet of doublets, td = triplet of doublets, m = multiplet, br = broad. Diffusion ordered NMR spectroscopy (DOSY) data were measured at 295 K with a Bruker Avance III HD 600MHz spectrometer and a 5 mm BBFO probe containing a z-axis gradient coil with a maximum gradient strength of 50 G cm^{-1}.

Mass spectrometry

High-resolution mass spectra (ESI) were recorded on a microTOF focus instrument (Bruker Daltronik GmbH).

Optical spectroscopy

For all spectroscopic measurements, spectroscopic grade solvents (Uvasol®) were used. The absorption spectra were recorded on JASCO V-670 or V-770 UV/vis-NIR spectrophotometers. The spectral band width and the scan rate were 1 nm and 400 nm min^{-1}, respectively. Stock solutions in $CHCl_3$ or 1,1,2,2-tetrachloroethane (TCE) were accurately freshly prepared for all measurements and continuously diluted for absorption measurements by taking into account the solubility and the absorbance. The UV/vis-NIR measurements were performed in quartz cell cuvettes with path lengths of 0.1, 1.0, 5.0, 10.0 and 100.0 mm. For temperature-dependent measurements, absorption spectra have been corrected for the density change. Fluorescence spectra were recorded on a FLS 980 Edinburgh fluorescence spectrometer. Fluorescence quantum yields were determined by a calibrated integrating sphere system (C9920, Hamamatsu, Japan). Time-resolved measurements were performed with a ps laser diode at 670 nm and a TCSPC detection unit.

Atomic force microscopy (AFM)

AFM measurements were performed under ambient conditions using a Bruker Multimode 8 SPM system operating in tapping mode in air. Silica cantilevers (OMCL-AC200TS, Olympus) with a resonance frequency of ~150 kHz and a spring constant of ~10 Nm^{-1} were used. The samples were prepared by spin-coating of solutions in toluene/TCE mixture (98:2, $c = 2 \times 10^{-5}$ M) onto highly ordered pyrolytic graphite (HOPG), silicon waver (SiO_x) or mica with 2000 rpm.

Computational Studies

Geometry optimization was performed for **BisSQ1** on the level of density functional theory (DFT) using the B3LYP functional[S1, S2] in combination with the 6-31G* basis set[S3] as implemented in the Gaussian 09 program package.[S4]

2. Synthesis and characterizations

Synthesis of compound **3**

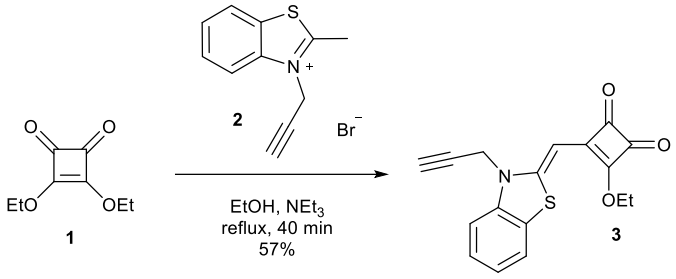

2-Methyl-3-propargylbenzothiazolium bromide (**2**) (839 mg, 3.13 mmol) was dissolved in 5.5 mL ethanol and 1.4 mL triethylamine. 1,2-diethoxycyclobutenedione (**1**) (0.53 mL, 3.7 mmol) was then added dropwise. The mixture was heated to reflux for 40 minutes. Afterwards, the reaction was cooled down to room temperature and the solvent was removed under reduced pressure. The crude product was purified by column chromatography (silica gel, eluent: pure CH_2Cl_2 to CH_2Cl_2/EtOAc 92:8) to obtain **3** as a yellow solid (554 mg, 1.78 mmol, 57%).

^{1}H NMR (400 MHz, DMSO-d_6): δ = 7.82 (dd, J = 8.0, 1.0 Hz, 1H), 7.51 (d, J = 8.0, 1H), 7.42 (td, J = 7.4, 1.0 Hz, 1H), 7.23 (t, J = 7.4 Hz, 1H), 5.68 (s, 1H), 5.11 (d, J = 2.4 Hz, 2H), 4.76 (q, J = 7.0 Hz, 2H), 3.46 (t, J = 2.4 Hz, 1H), 1.44 (t, J = 7.0 Hz, 3H) ppm.

^{13}C NMR (101 MHz, DMSO-d_6): δ = 192.2, 185.8, 185.3, 172.1, 158.3, 140.1, 127.2, 125.6, 123.8, 122.6, 111.8, 80.1, 76.9, 76.1, 69.5, 34.7, 15.7 ppm.

HRMS (ESI, pos. mode, MeOH): m/z: 334.05024 $[M+Na]^+$ (calcd. for $C_{17}H_{13}NNaO_3S^+$: 334.05084).

Mp: > 200 °C (decomp.)

Synthesis of compound **4**

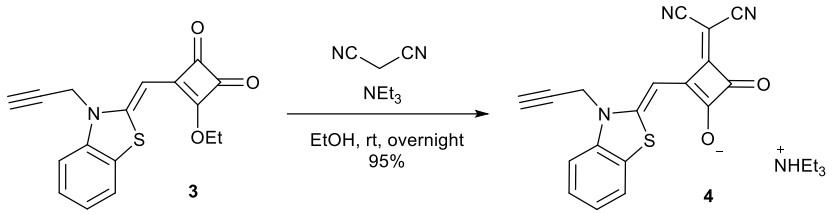

Compound **3** (491 mg, 1.58 mmol) was dissolved in 300 mL ethanol and malononitrile (522 mg, 7.90 mmol) was added while stirring. Triethylamine (1.1 mL, 7.9 mmol) was added dropwise. The mixture was stirred at room temperature overnight. The solvent was removed under reduced pressure and the solid was washed with diethyl ether to yield a dark orange powder (651 mg, 1.51 mmol, 95%).

^{1}H NMR (400 MHz, DMSO-d_6): δ = 7.65 (d, J = 7.3 Hz, 1H), 7.31 – 7.29 (m, 2H), 7.11 – 7.06 (m, 1H), 5.94 (s, 1H), 4.76 (d, J = 2.1 Hz, 2H), 3.37 (t, J = 2.3 Hz, 1H), 3.09 (m, 6H), 1.17 (t, J = 7.2 Hz, 9H) ppm.

^{13}C NMR (101 MHz, DMSO-d_6): δ = 191.1, 185.8, 174.4, 167.5, 152.4, 140.5, 126.6, 125.8, 122.6, 122.0, 118.9, 118.3, 110.5, 82.6, 79.2, 76.8, 75.5, 45.8, 34.2, 8.7 ppm.

HRMS (ESI, neg. mode, MeCN/$CHCl_3$): m/z: 330.03208 $[M-NHEt_3]^-$ (calcd. for $C_{18}H_8N_3O_2S^-$: 330.03427).

Mp: > 200 °C (decomp.)

Synthesis of compound **5a**

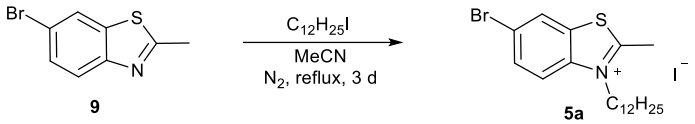

6-Bromo-2-methylbenzothiazole (**9**) (4.4 g, 19 mmol) and 1-iodododecane (14 mL, 57 mmol) was dissolved in 10 mL acetonitrile under nitrogen atmosphere and stirred during reflux for three days. After the reaction mixture was cooled down to room temperature, the solvent was removed under reduced pressure. The resulting residue was subsequently washed with ethyl acetate and diethyl ether to yield a yellow viscous material (2.5 g, 4.8 mmol, 25%). The synthesis was continued without further purification.

Synthesis of compound **6a**

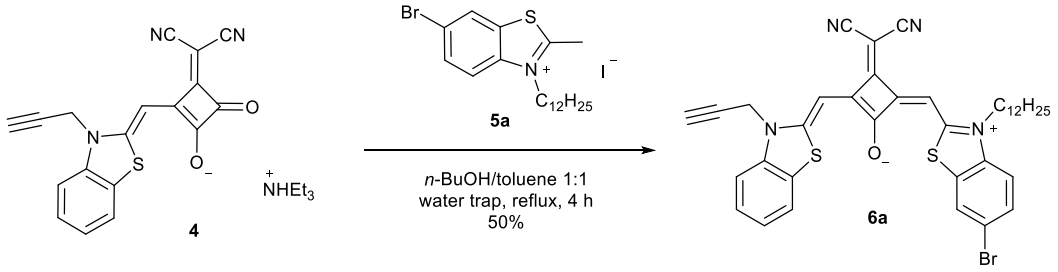

Compound **4** (35.6 mg, 82.0 µmol) and **5a** (88.0 mg, 168 µmol) were mixed in 2 mL *n*-butanol and 2 mL toluene and heated to reflux with a water-removing Dean-Stark apparatus for 4 h. Then the reaction mixture was cooled to room temperature and the solvent was removed under reduced pressure. The crude product was purified by column chromatography (silica gel, eluent: pure $CHCl_3$) to obtain a dark green solid. The solid was further washed with methanol. The solid was collected and dried to give a dark green powder (29.0 mg, 40.8 µmol, 50%).

^{1}H NMR (400 MHz, $CDCl_3$): δ = 7.65 (d, *J* = 1.8 Hz, 1H), 7.57 (dd, *J* = 8.0, 1.2 Hz, 1H), 7.53 (dd, *J* = 8.7, 1.8 Hz, 1H), 7.46 (td, *J* = 8.0, 1.2 Hz, 1H), 7.30 (m, 2H), 7.09 (d, *J* = 8.7 Hz, 1H), 6.40 (s, 1H), 6.38 (s, 1H), 4.84 (d, *J* = 2.4 Hz, 2H), 4.11 (t, *J* = 7.8 Hz, 2H), 2.46 (t, *J* = 2.4 Hz, 1H), 1.83 (quint, *J* = 7.8 Hz, 2H), 1.48 – 1.41 (m, 2H), 1.39 – 1.21 (m, 16H), 0.87 (t, *J* = 7.0 Hz, 3H) ppm.

^{13}C NMR (151 MHz, $CDCl_3$): δ = 174.2, 165.2, 164.7, 163.1, 160.8, 160.4, 140.17, 140.15, 130.9, 130.4, 128.2, 127.8, 125.1, 124.9, 122.5, 118.7, 118.5, 117.8, 113.3, 112.0, 87.9, 87.6, 75.4, 74.3, 47.4, 41.5, 36.0, 32.1, 29.75, 29.74, 29.65, 29.54, 29.49, 29.43, 27.7, 26.9, 22.9, 14.3 ppm.

HRMS (ESI, pos. mode, MeCN/$CHCl_3$): *m*/*z*: 708.1576 $[M]^+$ (calcd. for $C_{38}H_{37}BrN_4OS_2^+$: 708.1587).

Mp: > 225 °C (decomp.)

Synthesis of compound **6b**

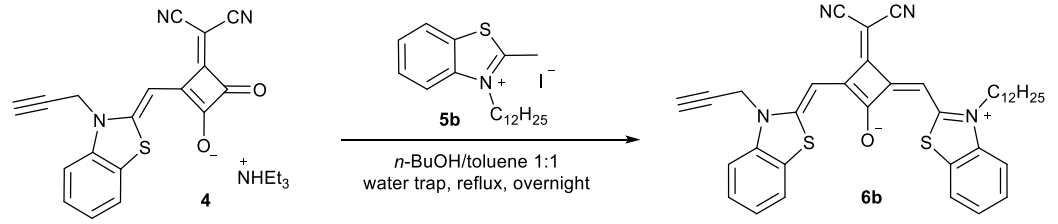

Compound **4** (202 mg, 467 µmol) and 2-methyl-3-dodecylbenzothiazolium iodide (**5b**) (473 mg, 1.06 mmol) were mixed in 15 mL *n*-butanol and 15 mL toluene and heated to reflux with

a water-removing Dean-Stark apparatus overnight. Then the reaction mixture was cooled to room temperature and the solvent was removed under reduced pressure. The crude product was purified by column chromatography (silica gel, eluent: pure $CHCl_3$) and the obtained solid was washed with methanol. The solid was collected and dried to give a dark green powder. This compound was applied for the next step without further purification.

Synthesis of compound **7**

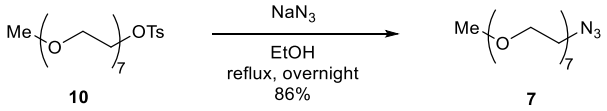

Hepta(ethylene glycol) monotosyl monomethyl ether (1.54 g, 3.11 mmol), and sodium azide (1.01 g, 15.6 mmol) were dissolved in 15 mL EtOH and heated to reflux overnight. After the reaction mixture was cooled down to room temperature, the solvent was removed under reduced pressure. The crude mixture was dissolved in CH_2Cl_2 (100 mL) and extracted with water (20 mL × 2) and brine (20 mL × 1). The combined organic layers were dried over $MgSO_4$ and evaporated to obtain a yellow oil (0.97 g, 2.7 mmol, 86%).

^{1}H NMR (400 MHz, $CDCl_3$): δ = 3.68 – 3.63 (m, 24H), 3.55 – 3.53 (m, 2H), 3.38 (t, J = 5.2 Hz, 2H), 3.37 (s, 3H) ppm.
^{13}C NMR (101 MHz, $CDCl_3$): δ = 72.1, 70.83, 70.80, 70.76, 70.74, 70.71, 70.65, 70.2, 59.2, 50.8 ppm.
HRMS (ESI, pos. mode, MeCN/$CHCl_3$): *m/z*: 388.20575 $[M+Na]^+$ (calcd. for $C_{15}H_{31}N_3NaO_7^+$: 388.20542).

Synthesis of compound **8a**

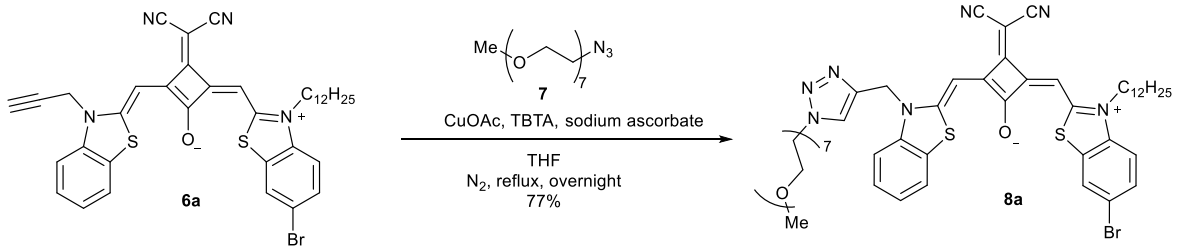

Copper (I) acetate (0.54 mg, 4.4 µmol) and sodium ascorbate (17 mg, 88 µmol) were suspended in 1 mL THF and stirred under nitrogen atmosphere for ca. 15 minutes until the color turned green. Precursors **6a** (15.7 mg, 22 µmol) and **7** (20.2 mg, 55 µmol) were dissolved in 1 mL THF and TBTA (4.7 mg, 8.8 µmol) and the Cu(I) catalyst solution were added. The reaction

mixture was then heated to reflux overnight under nitrogen atmosphere. Inorganic salts were filtered off and THF was removed under reduced pressure. Preparative recycling GPC ($CHCl_3$/MeOH = 9:1) was applied to isolate the pure product **8a** as a dark green solid (18.4 mg, 17 µmol, 77%).

^{1}H NMR (400 MHz, $CDCl_3$): δ = 8.37 (s, 1H), 7.94 (d, *J* = 8.3 Hz, 1H), 7.63 (d, *J* = 1.9 Hz, 1H), 7.57 – 7.49 (m, 3H), 7.31 (t, *J* = 7.5 Hz, 1H), 7.05 (d, *J* = 8.6 Hz, 1H), 6.43 (s, 1H), 6.31 (s, 1H), 5.39 (s, 2H), 4.56 (t, *J* = 5.3 Hz, 2H), 4.07 (t, *J* = 7.5 Hz, 2H), 3.91 (t, *J* = 5.3 Hz, 2H), 3.64 – 3.61 (m, 22 H), 3.55 – 3.52 (m, 2H), 3.37 (s, 3H), 1.82 (quint, *J* = 7.4 Hz, 2H), 1.48 – 1.40 (m, 2H), 1.37 – 1.25 (m, 16H), 0.87 (t, *J* = 6.8 Hz, 3H) ppm.
^{13}C NMR (101 MHz, CD_2Cl_2): δ = 173.8, 164.8, 164.4, 162.5, 161.1, 160.4, 141.3, 140.6, 140.0, 130.8, 130.6, 128.3, 128.0, 125.4, 125.3, 125.0, 122.4, 119.7, 118.6, 117.5, 114.0, 113.7, 113.5, 87.4, 72.2, 70.95, 70.86, 70.83, 70.81, 70.76, 70.7, 69.5, 59.0, 50.8, 47.6, 42.1, 32.3, 30.1, 30.0, 29.92, 29.87, 29.74, 29.66, 27.7, 27.2, 23.1, 14.3 ppm.
HRMS (ESI, pos. mode, MeCN/$CHCl_3$): *m*/*z*: 1073.37388 $[M]^+$ (calcd. for $C_{53}H_{68}BrN_7O_8S_2^+$: 1073.37487).
Mp: 174 – 175 °C.

Synthesis of compound **SQ1**

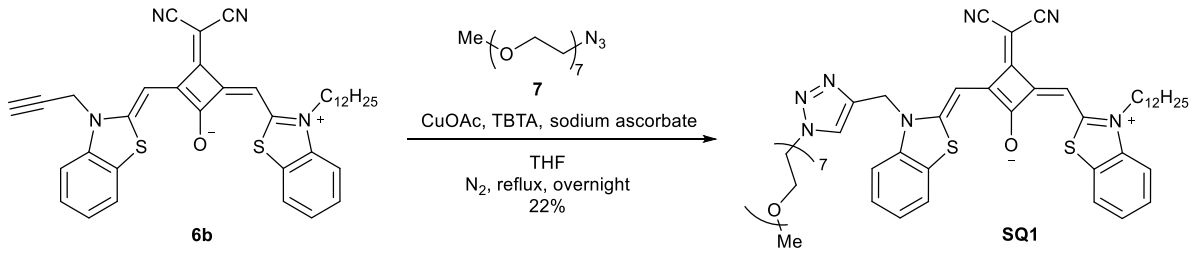

Copper (I) acetate (2.43 mg, 19.8 µmol) and sodium ascorbate (78.5 mg, 396 µmol) were suspended in 3 mL THF and stirred under nitrogen atmosphere for ca. 15 minutes until the color turned green. Precursors **6b** (62 mg, 99 µmol) and **7** (72.3 mg, 198 µmol) were dissolved in 10 mL THF, and TBTA (21.0 mg, 39.6 µmol) and the Cu(I) catalyst solution were added. The reaction mixture was stirred under reflux overnight under nitrogen atmosphere. Inorganic salts were filtered off and THF was removed under reduced pressure. Preparative recycling GPC ($CHCl_3$/MeOH = 9:1) was applied to isolate the pure product **SQ1** as a dark green solid (22.3 mg, 22.3 µmol, 22%).

^{1}H NMR (400 MHz, $CDCl_3$): δ = 8.36 (s, 1H), 7.90 (d, J = 8.3 Hz, 1H), 7.60 – 7.43 (m, 4H), 7.31 – 7.24 (m, 3H), 6.39 (s, 1H), 6.38 (s, 1H), 5.35 (s, 2H), 4.56 (t, J = 5.2 Hz, 2H), 4.15 (t, J = 7.5 Hz, 2H), 3.91 (t, J = 5.2 Hz, 2H), 3.65 – 3.61 (m, 22 H), 3.55 – 3.52 (m, 2H), 3.37 (s, 3H), 1.85 (quint, J = 7.4 Hz, 2H), 1.52 – 1.43 (m, 2H), 1.40 – 1.20 (m, 16H), 0.87 (t, J = 6.8 Hz, 3H) ppm.

^{13}C NMR (151 MHz, $CDCl_3$): δ = 174.3, 164.9, 163.7, 162.8, 161.4, 160.3, 141.2, 141.0, 139.8, 130.2, 129.9, 128.6, 127.9, 127.7, 125.2, 125.0, 124.9, 122.5, 122.1, 119.8, 118.8, 113.7, 112.3, 87.4, 86.5, 72.0, 70.8, 70.7, 70.6, 69.2, 59.2, 50.5, 47.2, 41.7, 40.5, 36.0, 32.1, 29.84, 29.80, 29.74, 29.66, 29.57, 29.51, 29.48, 29.44, 27.8, 27.0, 22.8, 14.3 ppm.

HRMS (ESI, pos. mode, MeCN/$CHCl_3$): m/z: 1018.45371 $[M+Na]^+$ (calcd. for $C_{53}H_{69}N_7NaO_8S_2^+$: 1018.45412).

Mp: 165 °C.

Synthesis of **BisSQ1**

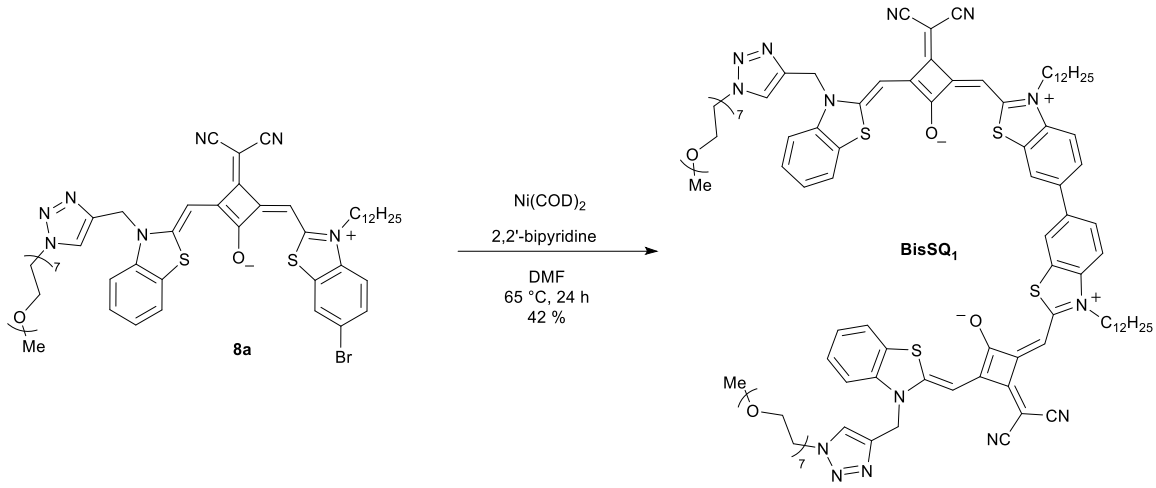

Squaraine **8a** (36.4 mg, 33.85 μmol), 2,2'-bipyridine (2.64 mg, 16.93 μmol), and bis-(1,5-cyclooctadiene)nickel(0) (4.66 mg, 16.93 μmol) were mixed in a Schlenk tube under N_2 atmosphere. Anhydrous DMF (10 mL) was added through a syringe into the reaction mixture and it was stirred at 65 °C for 24 hours. Afterwards, the reaction was cooled to room temperature and then diluted with 30 mL CH_2Cl_2. The solution was washed with water (30 mL ×3). The combined organic phase was dried over $MgSO_4$ and the solvent was removed under reduced pressure. Preparative recycling GPC ($CHCl_3$/MeOH = 9:1) was applied, giving pure **BisSQ1** as a dark green waxy solid (14.2 mg, 7.13 μmol, 42%).

^{1}H NMR (400 MHz, $CDCl_3$): δ = 8.37 (s, 2H), 7.92 (d, J = 8.2 Hz, 2H), 7.69 (d, J = 1.6 Hz, 2H), 7.59 (d, J = 8.6 Hz, 2H), 7.55 (d, J = 8.2 Hz, 2H), 7.50 (t, J = 8.0 Hz, 2H), 7.29 – 7.24 (m,

4H), 6.39 (s, 2H), 6.33 (s, 2H), 5.37 (s, 4H), 4.57 (t, *J* = 5.1 Hz, 4H), 4.13 (br, 4H), 3.92 (t, *J* = 5.1 Hz, 4H), 3.64 – 3.52 (m, 48H), 3.37 (s, 6H), 1.88 – 1.84 (m, 4H), 1.49 – 1.19 (m, 32H), 0.89 – 0.83 (m, 6H) ppm.

^{13}C NMR (151 MHz, $CDCl_3$): δ = 174.2, 164.3, 164.2, 162.8, 160.9, 160.4, 141.1, 140.8, 139.7, 136.2, 130.2, 129.9, 129.8, 128.0, 126.7, 126.6, 125.2, 124.3, 123.5, 122.1, 120.2, 119.7, 118.7, 113.9, 112.5, 87.5, 87.0, 72.1, 70.8, 70.73, 70.68, 70.65, 69.2, 59.2, 50.5, 47.3, 41.8, 40.6, 32.1, 29.85, 29.81, 29.76, 29.69, 29.60, 29.51, 29.49, 27.8, 27.0, 22.8, 14.3 ppm.

HRMS (ESI, pos. mode, MeCN/$CHCl_3$): *m*/*z*: 2011.8988 $[M+Na]^+$ (calcd. for $C_{106}H_{136}N_{14}NaO_{16}S_4$: 2011.9034).

Mp: > 285 °C (decomp.)

3. UV/vis absorption and fluorescence spectroscopy

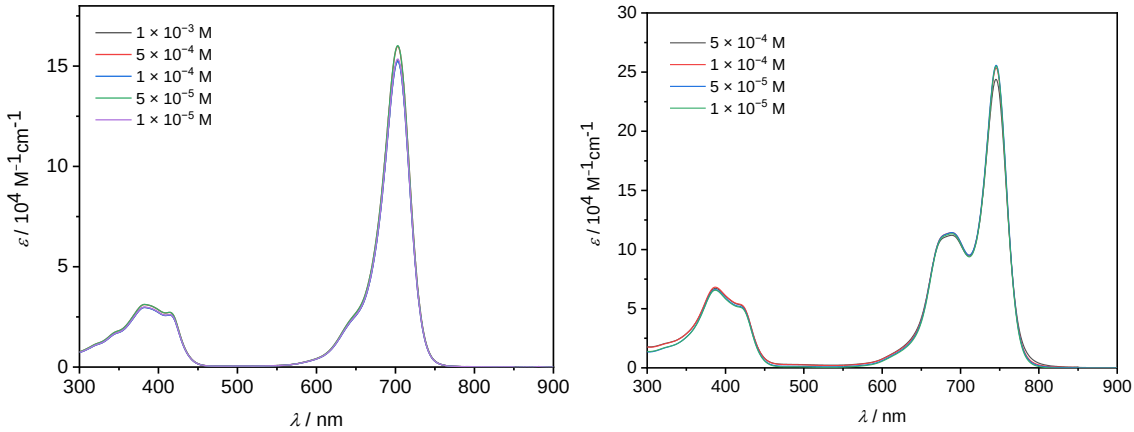

Figure S1. UV/vis absorption spectra of **SQ1** (left) and **BisSQ1** (right) in $CHCl_3$ at different concentrations at 25 °C.

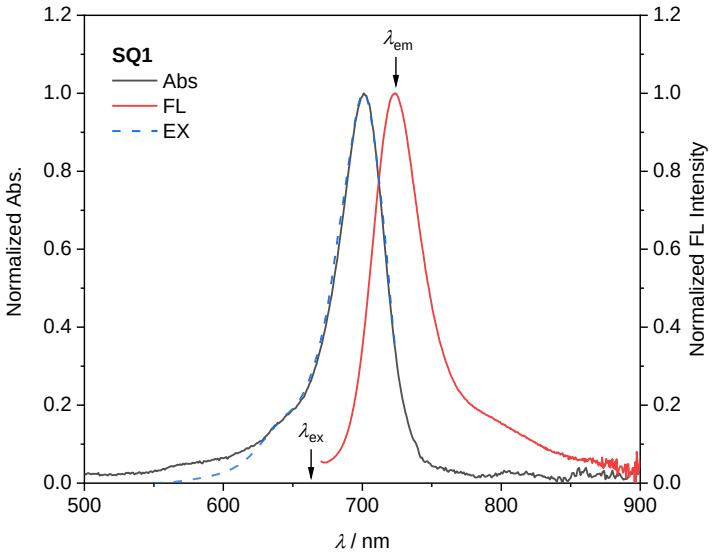

Figure S2. Normalized UV/vis (solid black line), fluorescence (solid red line, λ_{ex} = 660 nm) and excitation (dashed blue line, λ_{em} = 724 nm) spectra of **SQ1** in $CHCl_3$ at $c = 5\times10^{-6}$ M, 25 °C.

Determination of absolute fluorescence quantum yield

During the fluorescence quantum yield investigation of **SQ1** and **BisSQ1** utilizing an integrating sphere, strong reabsorption took place, which was identified by the broadening and decrease of the fluorescence intensity and the shift of the fluorescence maximum to lower wavelength upon dilution. The reabsorption contaminated spectrum were adjusted at the red edge to the reabsorption-free fluorescence spectrum (Figure S3) and the corrected absolute quantum yields were determined using the approach of Ahn *et al.*[S5]

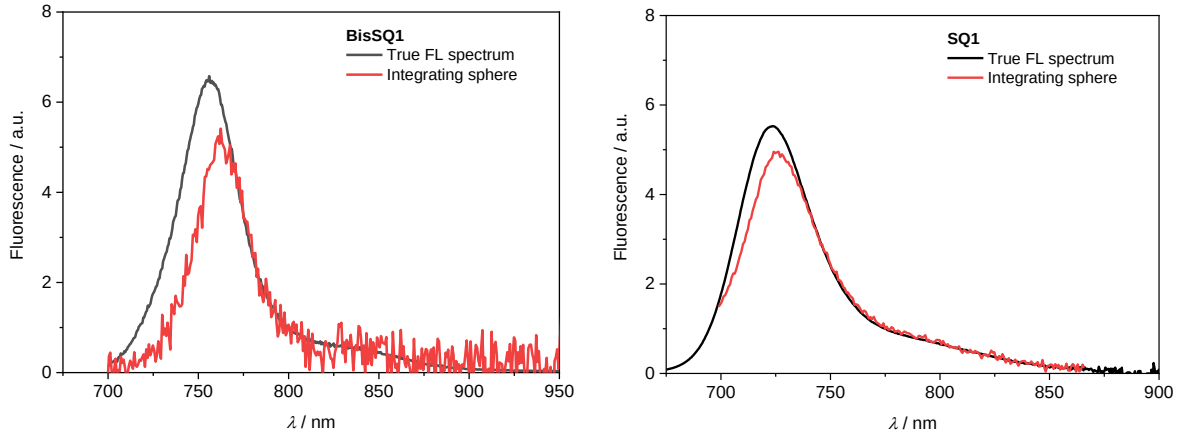

Figure S3. Left: Fluorescence spectrum of **BisSQ1** in $CHCl_3$ solution measured with the integrating sphere (c = 2 × 10^{-6} M, red line) adjusted to the red edge of the reabsorption-free spectrum (c = 2 × 10^{-6} M, black line). Right: Fluorescence spectrum of **SQ1** in $CHCl_3$ solution measured with the integrating sphere ($c = 5\times10^{-6}$ M, red line) adjusted to the red edge of the reabsorption-free spectrum ($c = 5\times10^{-6}$ M, black line).

4. Self-assembly studies

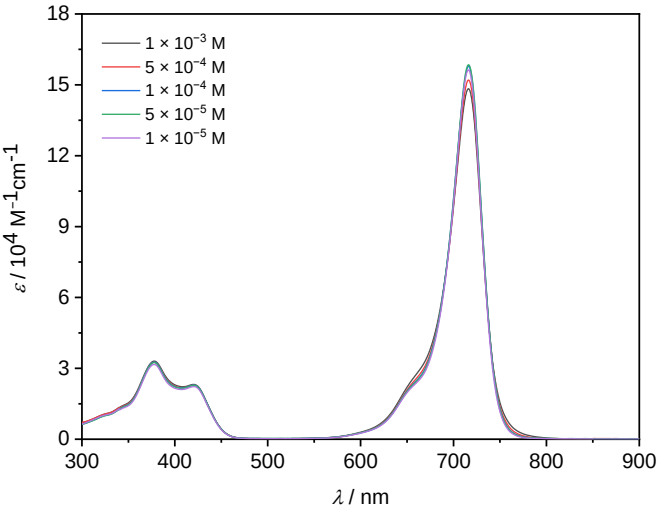

Figure S4. UV/vis absorption spectra of **SQ1** in toluene/TCE 98:2 at different concentrations at 25 °C (λ_{max} = 716 nm).

Data evaluation

For the thermodynamic analysis of the self-assembly processes, literature known procedures were applied. The temperature-dependent analyses were performed according to the procedures recently reported by Meijer, Schenning and Van der Schoot.[S6,S7] The equations used to fit the concentration-dependent UV/vis data are according to the monomer-dimer,[S8] isodesmic (equal-*K*)[S9] and the cooperative K_2/*K* model.[S10]

Determination of the degree of aggregation based on UV/vis data

The degree of aggregation α was calculated from the data obtained by concentration and temperature-dependent UV/vis measurements according to Equations (S1) and (S2)

$$\alpha(c) = \frac{\varepsilon(c)-\varepsilon_M}{\varepsilon_A-\varepsilon_M} \quad \text{(S1)}$$

$$\alpha(T) = \frac{\varepsilon(T)-\varepsilon_M}{\varepsilon_A-\varepsilon_M} \quad \text{(S2)}$$

where $\varepsilon(c)$ is the measured apparent absorption coefficient at concentration c, ε(T) is the measured apparent absorption coefficient at temperature T, and ε_M and ε_A are the respective absorption coefficients of the monomer (M) and fully aggregated state (A). ε_M and ε_A could be determined directly from the spectroscopic data at high and low concentrations and temperatures.

Nucleation-elongation Model of Meijer, Schenning and Van der Schoot[S6,S7]

In the elongation regime, the fraction of aggregated species (α_{agg}) can be defined by

$$\alpha_{agg} = \alpha_{SAT}\left(1 - exp\left[\frac{-\Delta H_e}{RT_e^2}(T - T_e)\right]\right) \quad \text{(S3)}$$

in which ΔH_e is the enthalpy corresponding to the aggregation (elongation) process, T the absolute temperature, T_e the elongation temperature, R the ideal gas constant and α_{SAT} is a parameter introduced to ensure that $\alpha_{agg}/\alpha_{SAT}$ does not exceed unity.

On the other hand, in the nucleation regime, α_{agg} can be defined by

$$\alpha_{agg} = K_a^{1/3} exp\left[\left(2/3K_a^{-1/3} - 1\right)\frac{\Delta H_e}{RT_e^2}(T - T_e)\right] \quad \text{(S4)}$$

where K_a is the dimensionless equilibrium constant of the activation step at the elongation temperature.

As presented in the main text, temperature-dependent UV/vis measurement of **BisSQ1** was carried out in a solvent mixture of toluene/1,1,2,2-tetrachloroethane (TCE) = 98:2 (*v*/*v*) from 282 K to 358 K at the concentration of 5×10^{-6} M. The heating process led to a transition from aggregated (λ_{max} = 886 nm) to monomeric (λ_{max} = 757 nm) species. However, under the measurement conditions, the fully aggregated state was not achieved. Thus, we could only determine the value of ε_M. For ε_A, a very concentrated solution of **BisSQ1** in toluene/TCE 98:2 at $c = 1.0 \times 10^{-3}$ M was prepared and measured separately at low temperatures, namely 278 and 283 K. Since both UV/vis absorption spectra looked identical (Figure S5), we assume **BisSQ1** to be fully aggregated at this condition. Hence, ε_A can be deduced from these spectra at the desired wavelength λ = 886 nm and thus the degree of aggregation α can be calculated in order to perform the analysis using the nucleation-elongation model[S3] (Figure 3 in the main text).

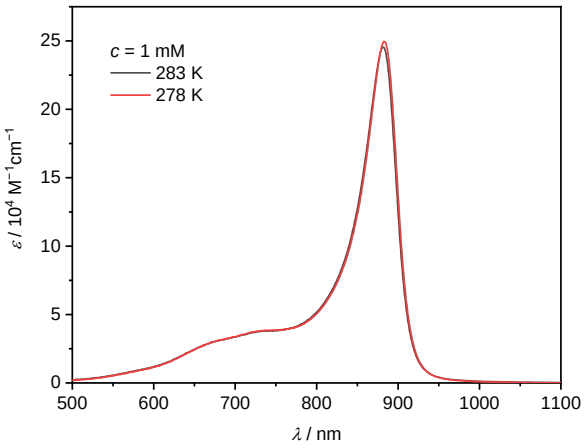

Figure S5. UV/vis spectra of **BisSQ1** in toluene/TCE 98:2 (*v*/*v*) at $c = 1.0 \times 10^{-3}$ M, 278 and 383 K.

Concentration-dependent UV/vis measurements were carried out to complement our investigation of the cooperative self-assembly process of **BisSQ1**. Therefore, **BisSQ1** solutions in a solvent mixture of toluene/$CHCl_3$ = 95:5 (*v*/*v*) from $c = 2 \times 10^{-7}$ M to 1×10^{-4} M at 25 °C were prepared and measured. $CHCl_3$ was used as an additive to increase the solubility of **BisSQ1** in order to cover a broad concentration range. As shown in Figure. S6, an increase of the concentration from $c = 2 \times 10^{-7}$ M to 1×10^{-4} M at 25 °C results in a transition from monomeric species (λ_{max} = 757 nm) to nearly totally aggregated species (λ_{max} = 886 nm). The degree of aggregation was calculated according to the experimental data extracted at 886 nm and plotted against the concentration (Figure S7). Indicated by the abrupt decrease of the apparent absorption at 739 nm, the monomer-dimer[S8] or isodesmic (equal-*K*)[S9] model failed to describe the aggregation process (Figure S7 left). By applying the cooperative K_2/K model[S10], a pronounced cooperativity of 0.08 with the elongation constant $K = 7.5 \times 10^5$ M^{-1} were yielded, which is in good agreement with the temperature-dependent measurements (Figure S7 right).

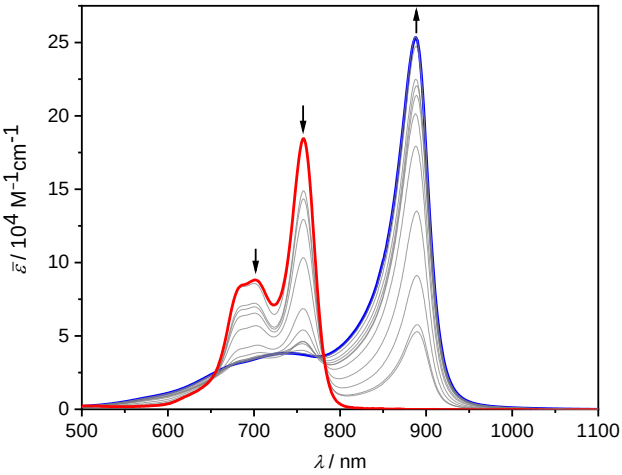

Figure S6. Concentration-dependent UV/vis spectra of **BisSQ1** in toluene/$CHCl_3$ 95:5 (*v*/*v*) at $c = 1.0 \times 10^{-4} – 2.0 \times 10^{-7}$ M, 25 °C. The arrows indicate the spectral changes with increasing concentration.

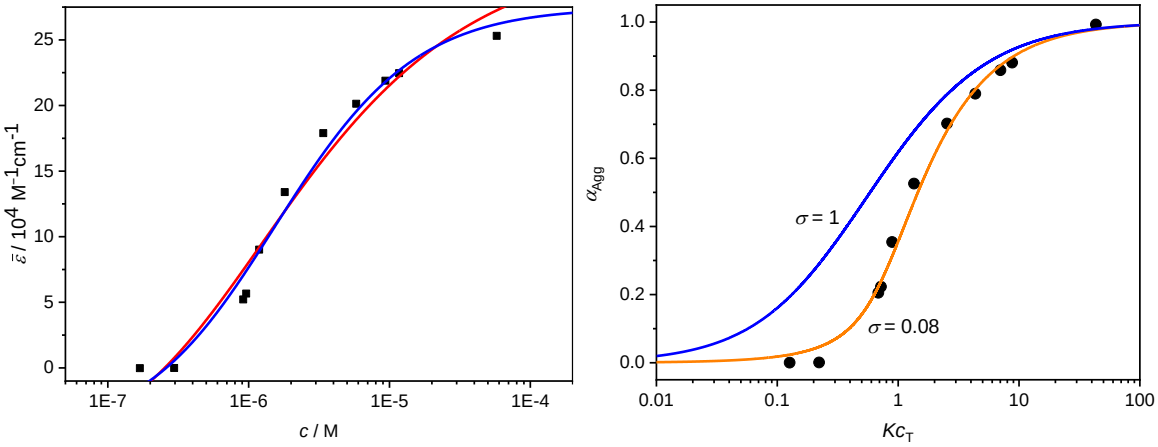

Figure S7. Left: apparent molar absorption at 886 nm as a function of concentration of **BisSQ1** in toluene/$CHCl_3$ 95:5 fitted with the monomer-dimer[S8] (red line, $r^2 = 0.9712$) and the isodesmic model[S9] (blue line, $r^2 = 0.9833$). Right: plot of fractions of aggregate against Kc_T and fitting with the cooperative K_2/K model[S10] with different σ values.

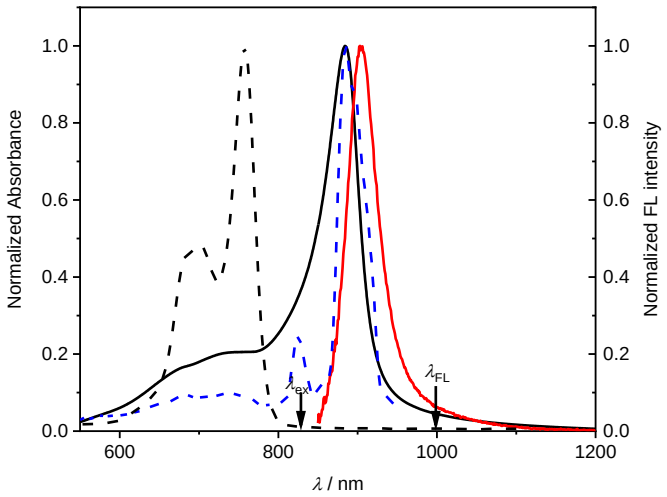

Figure S8. Normalized absorption (solid black line), fluorescence (solid red line) and excitation spectra (dashed blue line) of aggregated **BisSQ1** in toluene/$CHCl_3$ 95:5 (*v*/*v*) at $c = 6.0 \times 10^{-5}$ M, 25 °C and the absorption spectrum of **BisSQ1** in $CHCl_3$ at $c = 1 \times 10^{-5}$ M, 25 °C (dashed black line).

Table S1. Summarized absorption and fluorescence data of aggregated **BisSQ1** in toluene/$CHCl_3$ 95:5 (*v*/*v*) at $c = 6.0 \times 10^{-5}$ M, 25 °C.

λ_{max} (nm)	λ_{FL}[a] (nm)	$\Delta\tilde{\nu}_{Stokes}$ (cm^{-1})	FWHM (cm^{-1})
886	904	225	620

[a] λ_{ex} = 820 nm. Fluorescence spectrum was measured with a front-face setup (1 mm cell thickness) and the polarizer at magic angle; excitation spectrum was measured with a front-face setup (1 mm cell thickness) without polarizers.

5. DOSY NMR

DOSY NMR studies were performed in toluene-d_8 (Figure S9, the selected peaks (*) correspond to the proton signals of **BisSQ1**). In order to avoid the influence of convection effects due to temperature gradients in the coil of the probe, two different pulse sequences, a stimulated echo BPP-LED pulse sequence with sample rotation and a corresponding double stimulated echo pulse sequence without sample rotation were used. No differences in diffusion data obtained from the two pulse sequences were observed, which confirms the absence of convection effects. The diffusion coefficients were obtained by fitting the decay curves of the signal area versus the gradient strength with a monoexponential function. The decay curves with the respective fit and the resulting hydrodynamic radii are shown in Figure S10 a–d.

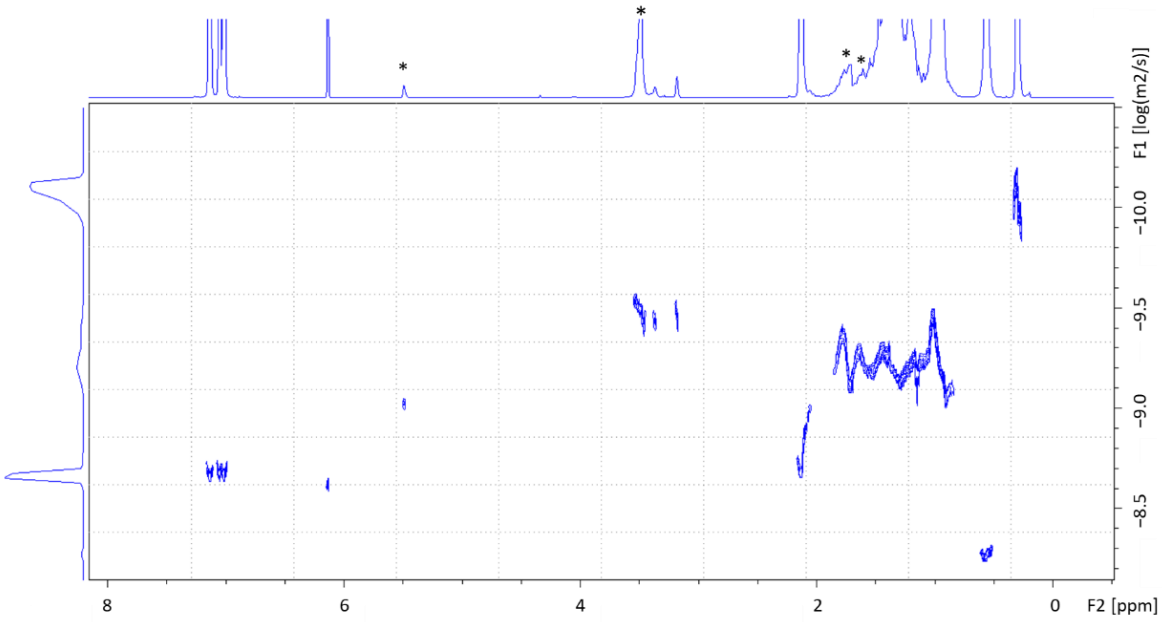

Figure S9. DOSY NMR spectrum of **BisSQ1** in toluene-d_8 ($c = 5 \times 10^{-4}$ M, 295 K, 600 MHz). The selected signals (*) correspond to the **BisSQ1** moieties.

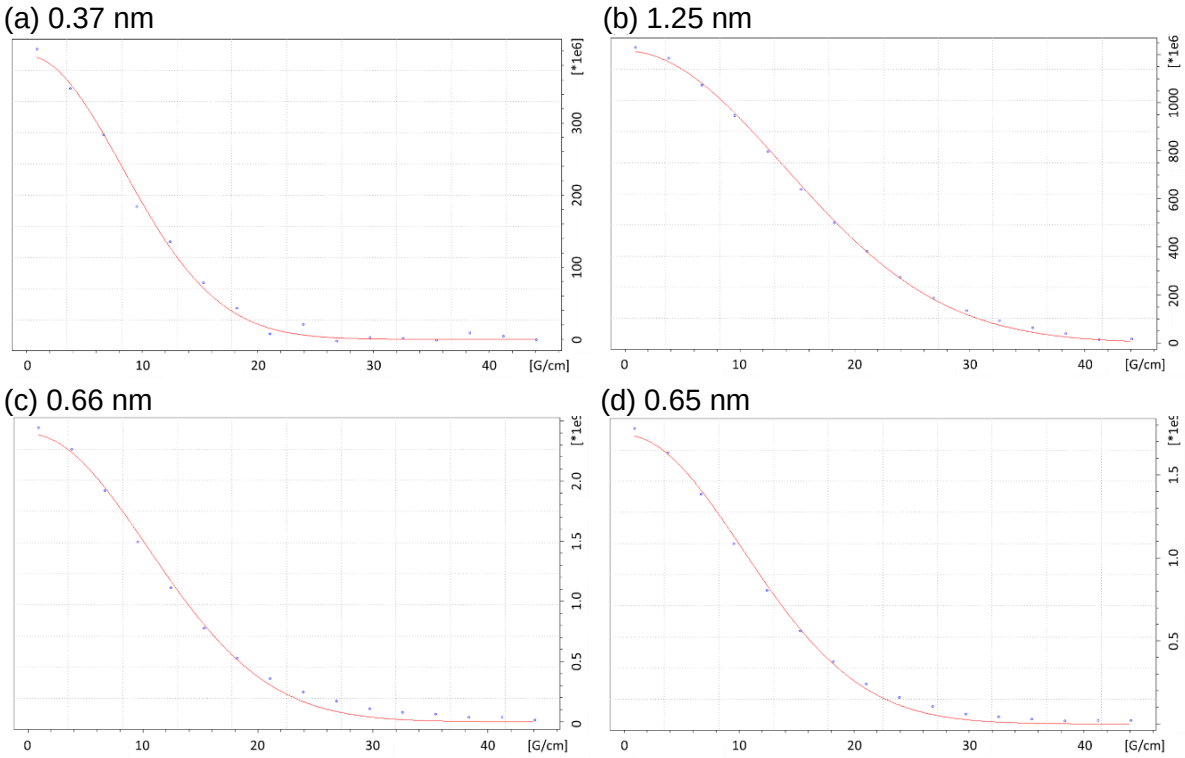

Figure S10. Decay curves and corresponding monoexponential fit for the selected signals as obtained from the Topspin fitting routine for **BisSQ1**. (a) 5.58 – 5.36 ppm, Diffusion coefficient = 9.88×10^{-10} m^2/s; (b) 3.60 – 3.43 ppm, Diffusion coefficient = 2.93×10^{-10} m^2/s; (c) 1.86 – 1.68 ppm, Diffusion coefficient = 5.50×10^{-10} m^2/s; (d) 1.68 – 1.55 ppm, Diffusion coefficient = 5.68×10^{-10} m^2/s. The corresponding hydrodynamic radii are given on the top of the respective decay curves.

Unfortunately, an unambiguous interpretation was not possible. The data showed different diffusion coefficients (which correspond to various hydrodynamic radii) for the different functional groups within the same molecule. This can be due to a distribution of sizes of the sheet-like aggregates in solution. The selected ^{1}H NMR signals may originate from aggregates of different size, thus causing a variation in the observed diffusion coefficient. Additionally, the strong aggregation and reduced mobility of some functional groups within the aggregate results in signal broadening and is the reason why only few signals of the aggregated species can be observed (Figure S9). The reported diffusion coefficients (see caption of Figure S10) were obtained from pseudo-2D measurements with the BPP-LED pulse sequence and converted to approximate radii by using the dynamic viscosity of toluene at 295 K. We also want to emphasize that the DOSY analysis and the corresponding equations are generally designed for spherical particles with a uniform size. In our case, we assume sheet-like structures (see AFM studies) and the growth of the aggregate cannot be controlled, resulting in an unknown size distribution.

6. AFM studies

The thin film consisting of the sheet-like structures was observed on hydrophobic silicon wafer (Figure S11 left) as well as on hydrophilic mica (Figure S11 right). The height of the sheets was measured to be 2.0 ± 0.2 nm. The width varies between 10 – 40 nm and the length is up to 200 nm. The observed dimensions are comparable with that of the sheet-like structures on HOPG, as described in the main text (Figure 4a and b).

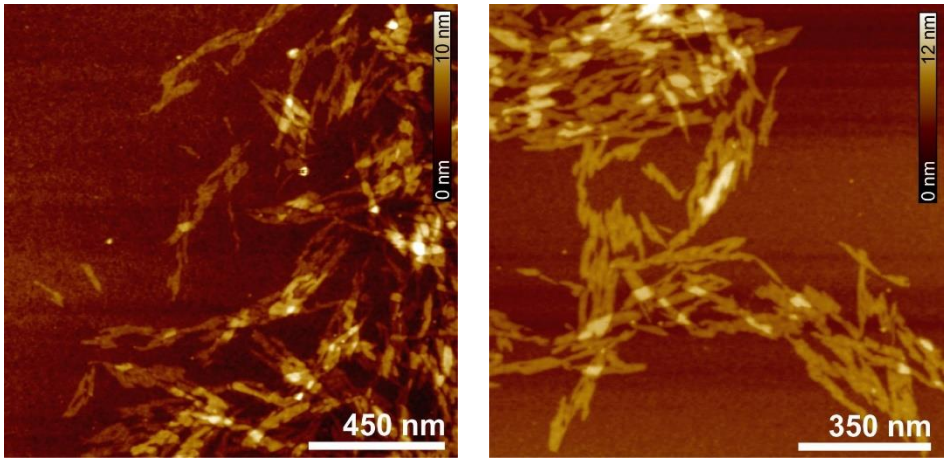

Figure S11. Height AFM images of sample **BisSQ1** prepared by spin-coating of toluene/TCE 98:2 (*v*/*v*) solution on SiO_x (left, *Z* scale is 10 nm); mica (right, *Z* scale is 12 nm.)

7. Proposed packing model

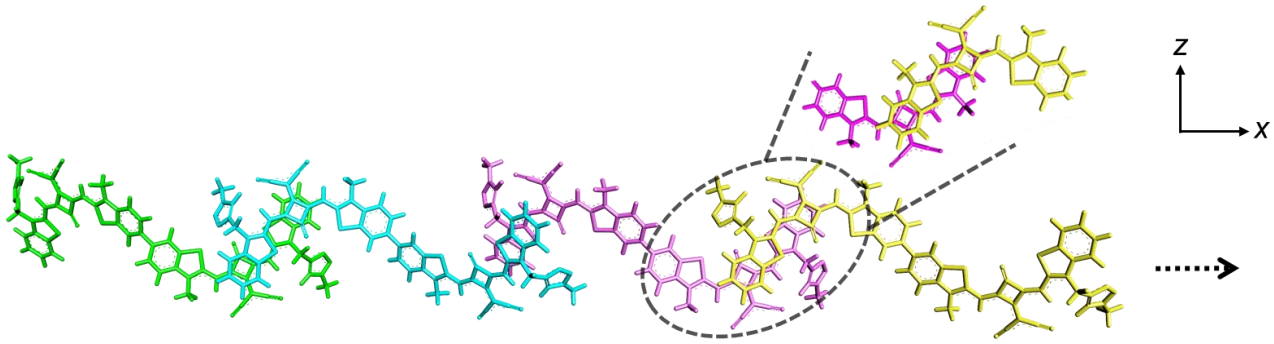

Figure S12. Proposed chromophore arrangement with each molecule coloured differently within the nanosheet of self-assembled **BisSQ1** simulated and visualized using the program suite *BIOVIA Materials Studio 2017R2*. The geometry of the monomers was optimized at the level of density functional theory (B3LYP/6-31G*). Dashed arrow shows the supramolecular polymerization in x-axis. (Side chains are neglected for simplicity.)

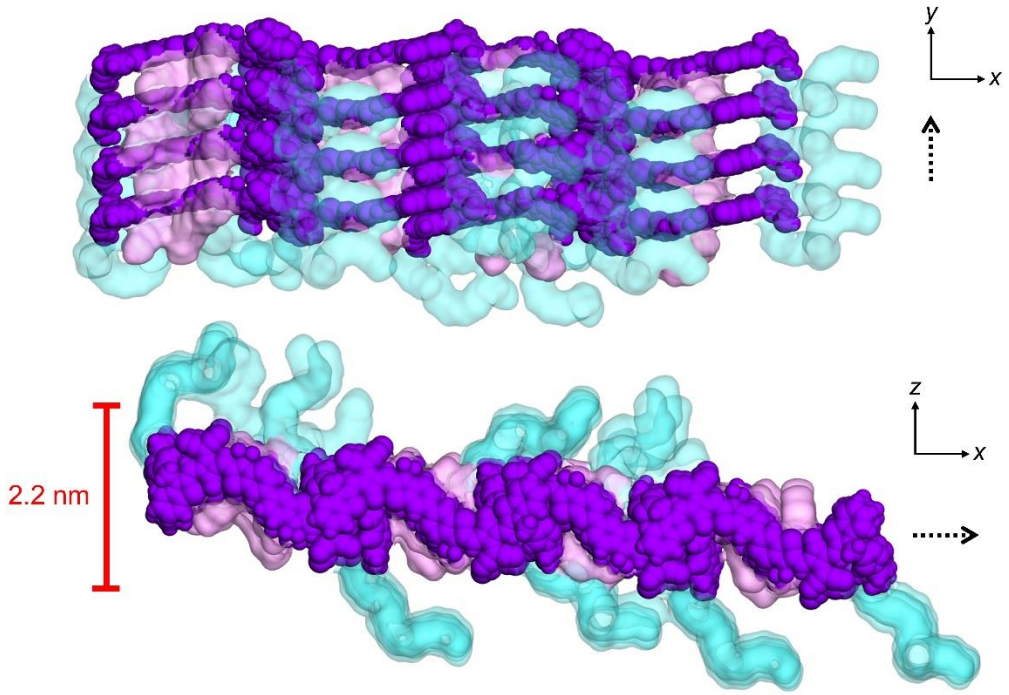

Figure S13. Proposed packing model of the nanosheets of self-assembled **BisSQ1**. Side view (top) and top view (bottom) of the nanosheet with the chromophores coloured in violet. The geometry of the individual chromophores was optimized at the level of density functional theory (B3LYP/6-31G*). Oligoethyleneglycol chains are colored in cyan and aliphatic chains in pale violet, respectively. The model was created and optimized using the program suite *BIOVIA Materials Studio 2017R2* with the Forcite module in combination with the force field COMPASSII. Dashed arrows show the direction of two-dimensional supramolecular polymerization.

8. NMR spectra

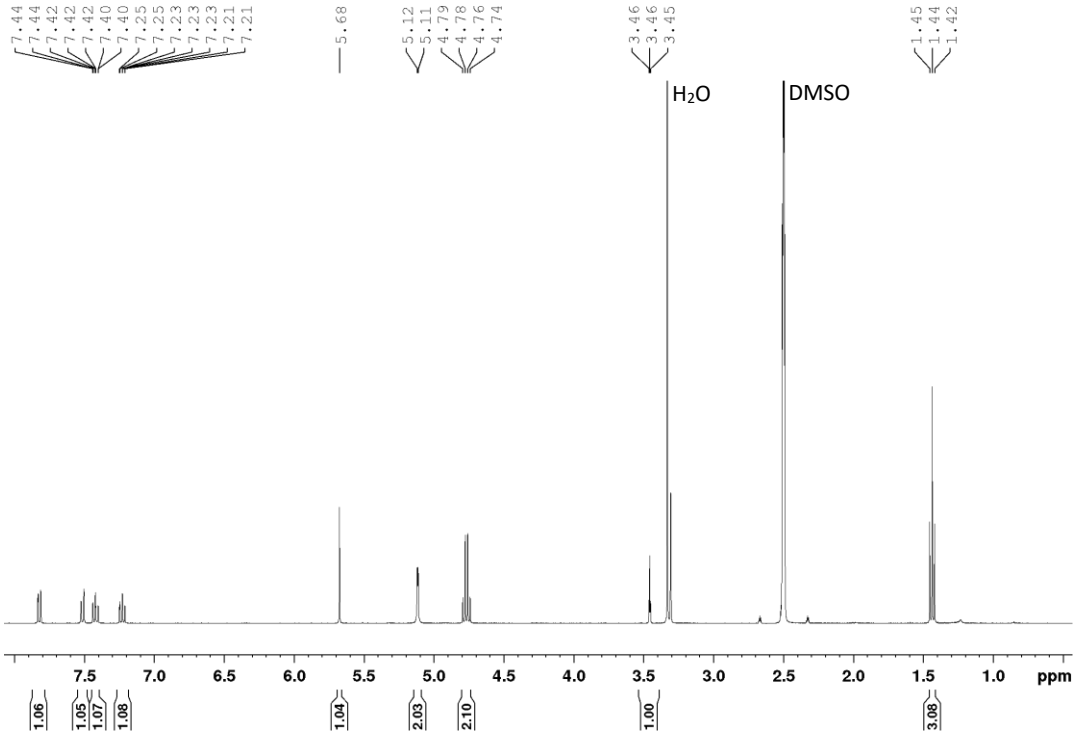

Figure S14. ^{1}H NMR (400 MHz, 295 K) spectrum of compound **3** in DMSO-d_6.

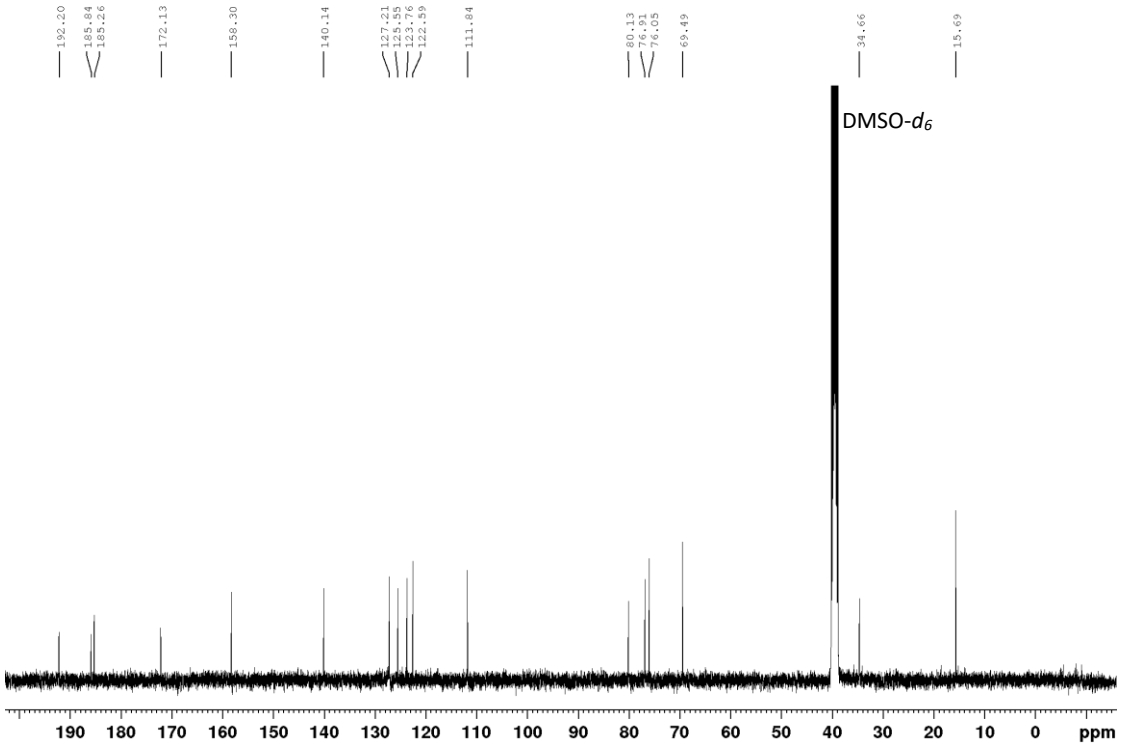

Figure S15. ^{13}C NMR (101 MHz, 295 K) spectrum of compound **3** in DMSO-d_6.

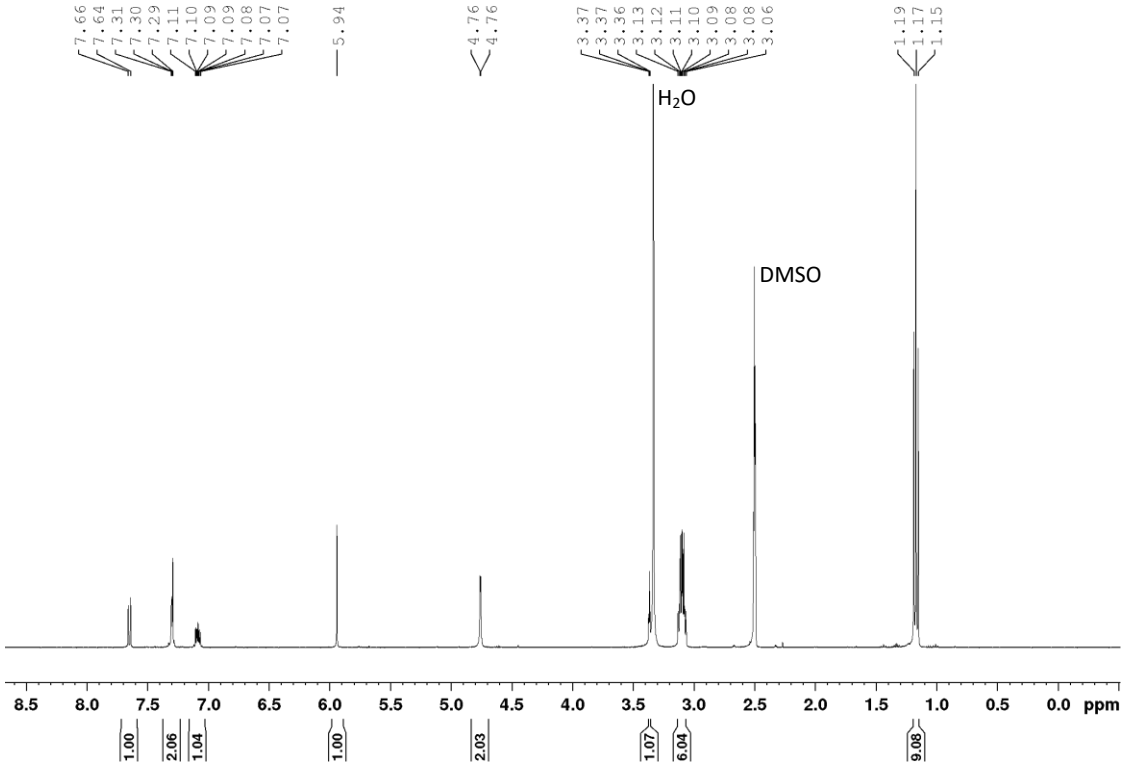

Figure S16. [1]H NMR (400 MHz, 295 K) spectrum of compound **4** in DMSO-d_6.

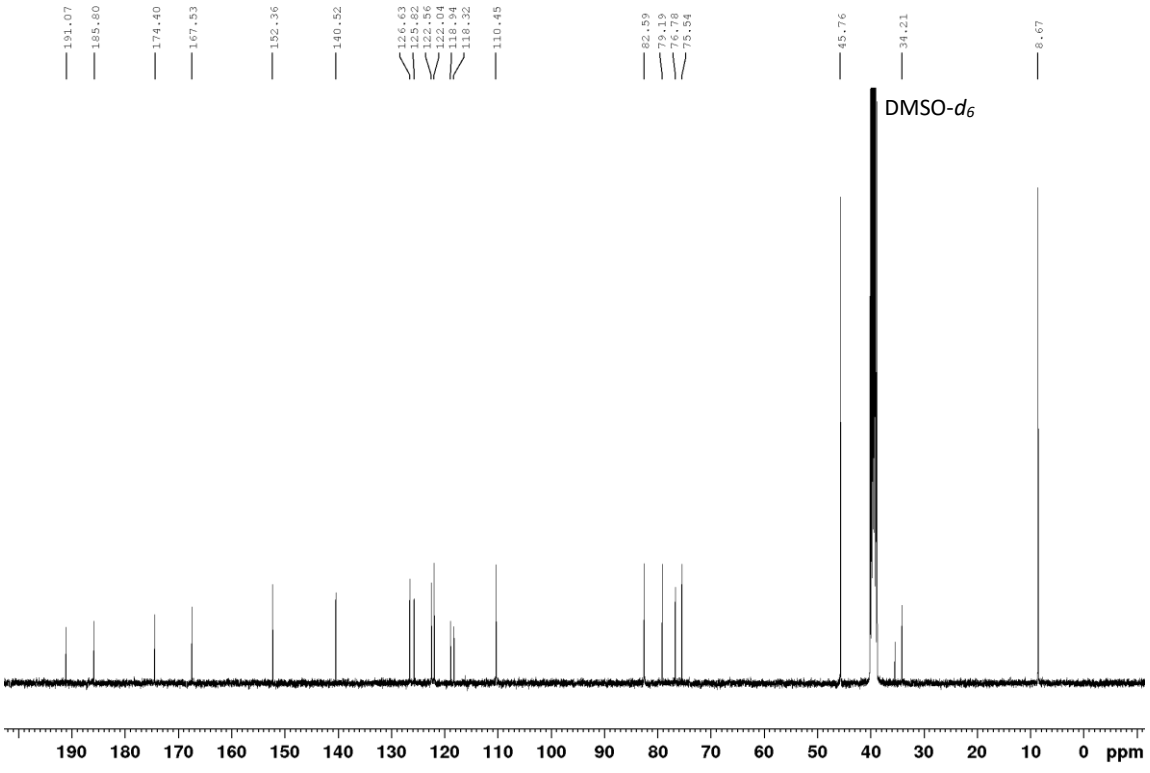

Figure S17. [13]C NMR (101 MHz, 295 K) spectrum of compound **4** in DMSO-d_6.

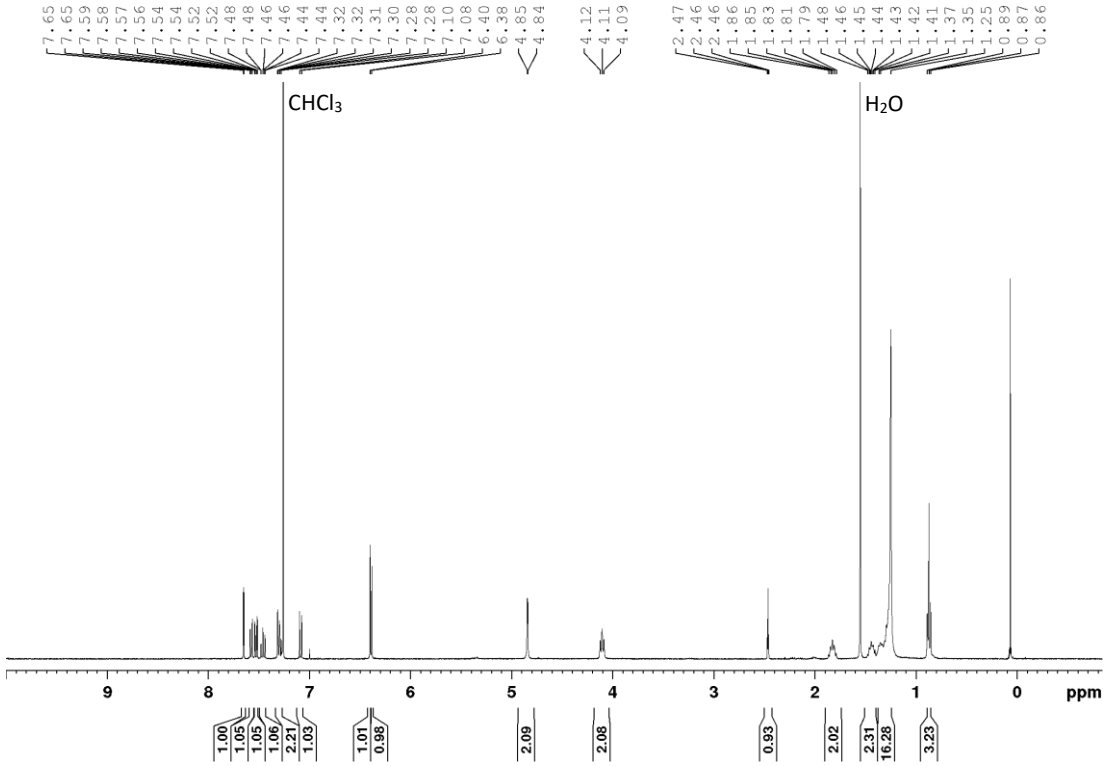

Figure S18. ^{1}H NMR (400 MHz, 295 K) spectrum of compound **6a** in $CDCl_3$.

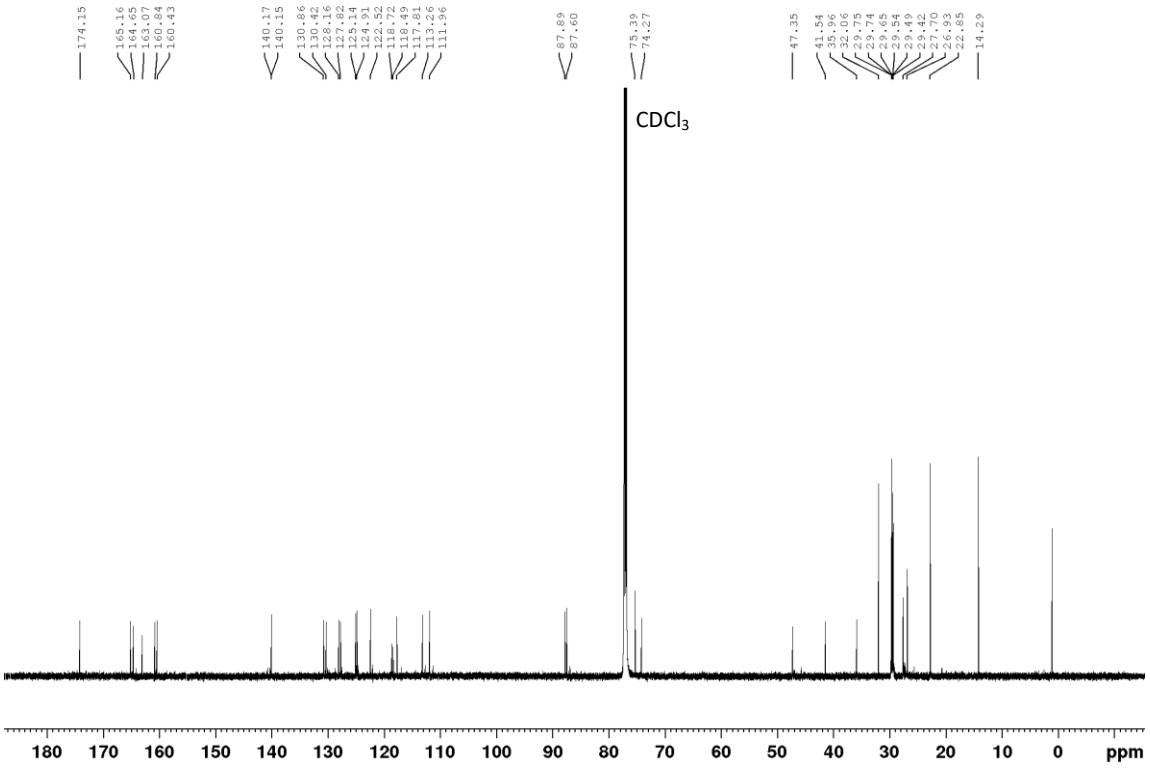

Figure S19. ^{13}C NMR (151 MHz, 295 K) spectrum of compound **6a** in $CDCl_3$.

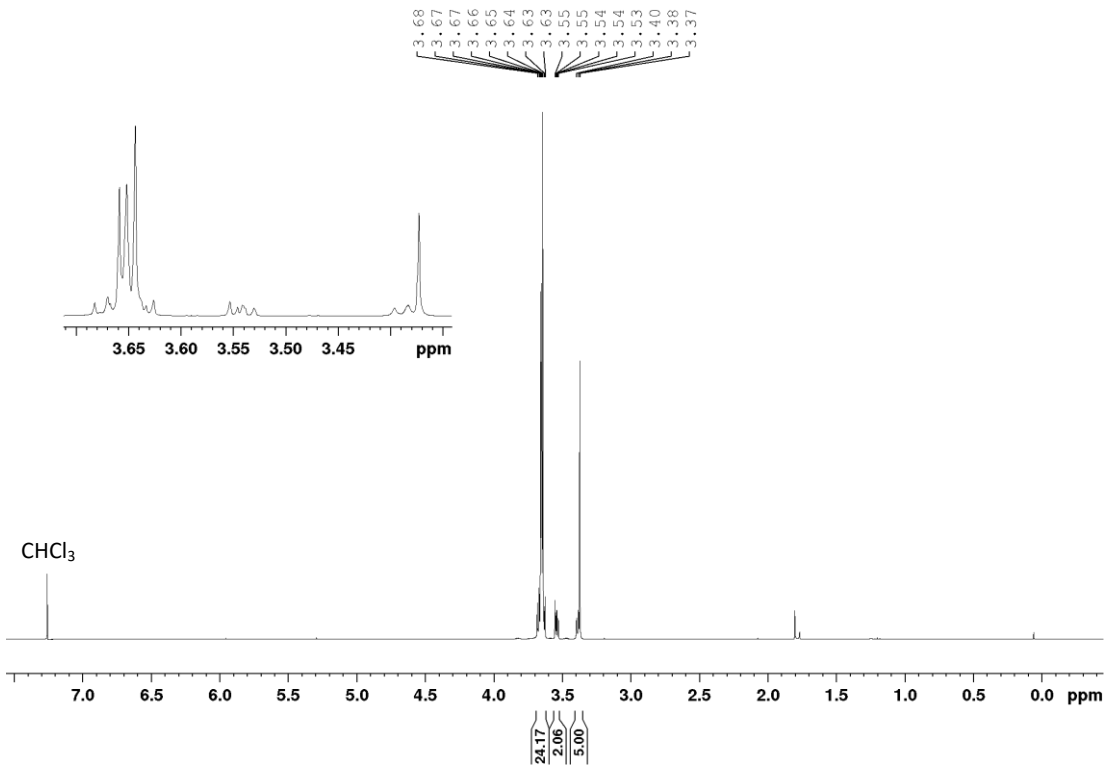

Figure S20. ^{1}H NMR (400 MHz, 295 K) spectrum of compound **7** in $CDCl_3$.

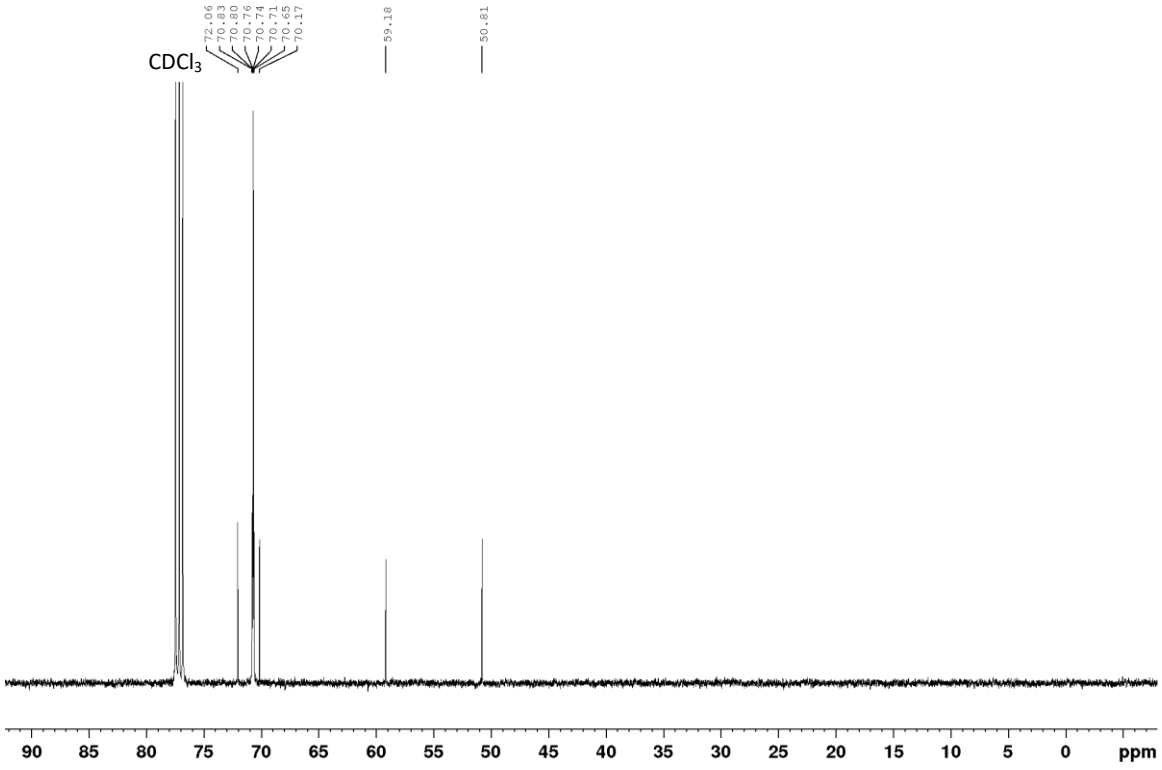

Figure S21. ^{13}C NMR (101 MHz, 295 K) spectrum of compound **7** in $CDCl_3$.

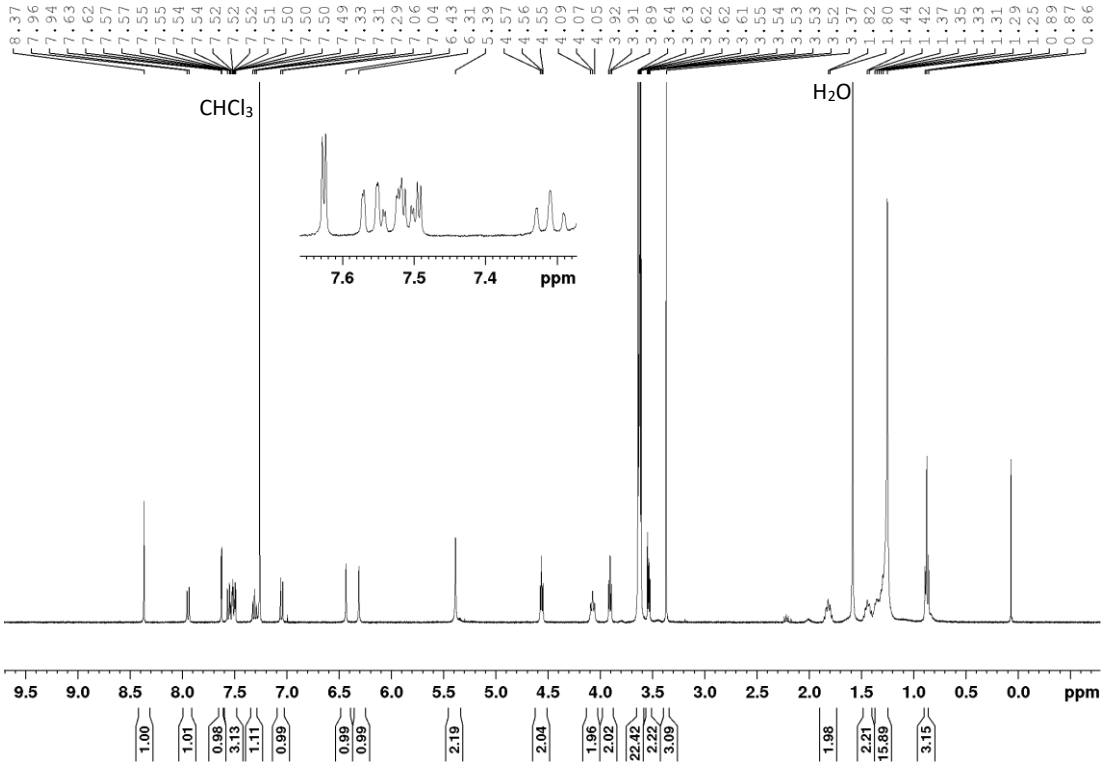

Figure S22. ^{1}H NMR (400 MHz, 295 K) spectrum of compound **8a** in $CDCl_3$.

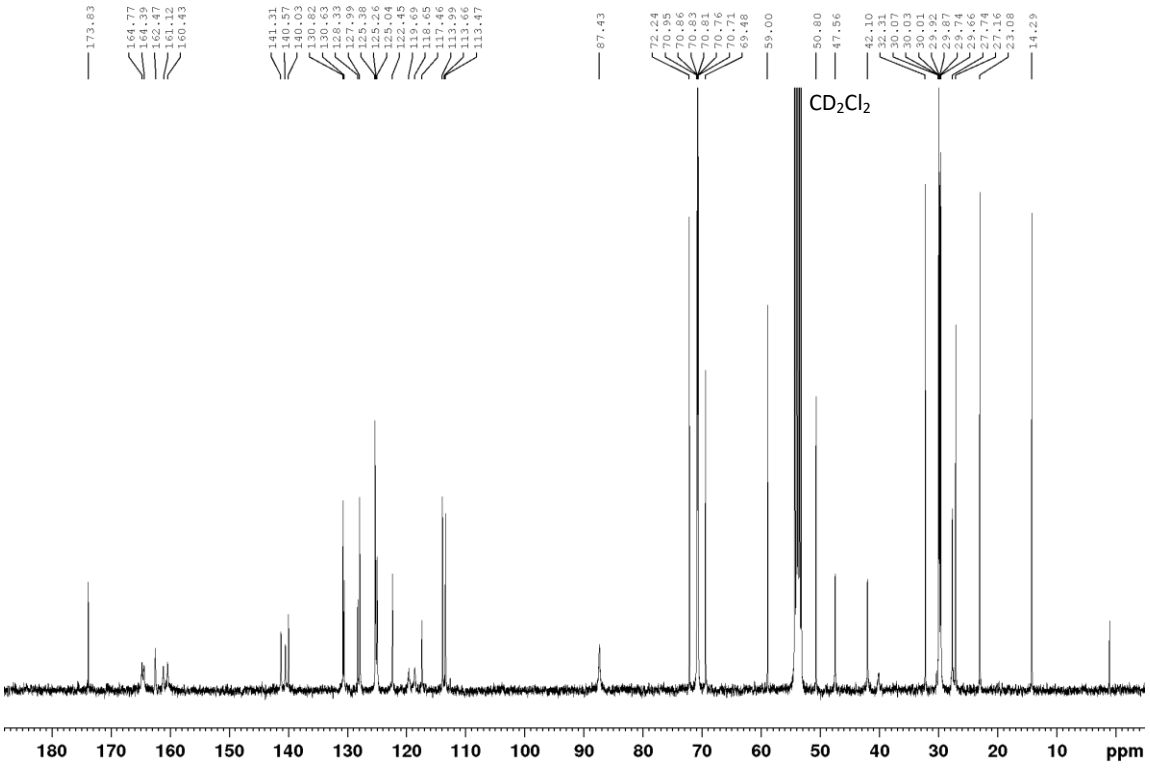

Figure S23. ^{13}C NMR (101 MHz, 295 K) spectrum of compound **8a** in CD_2Cl_2.

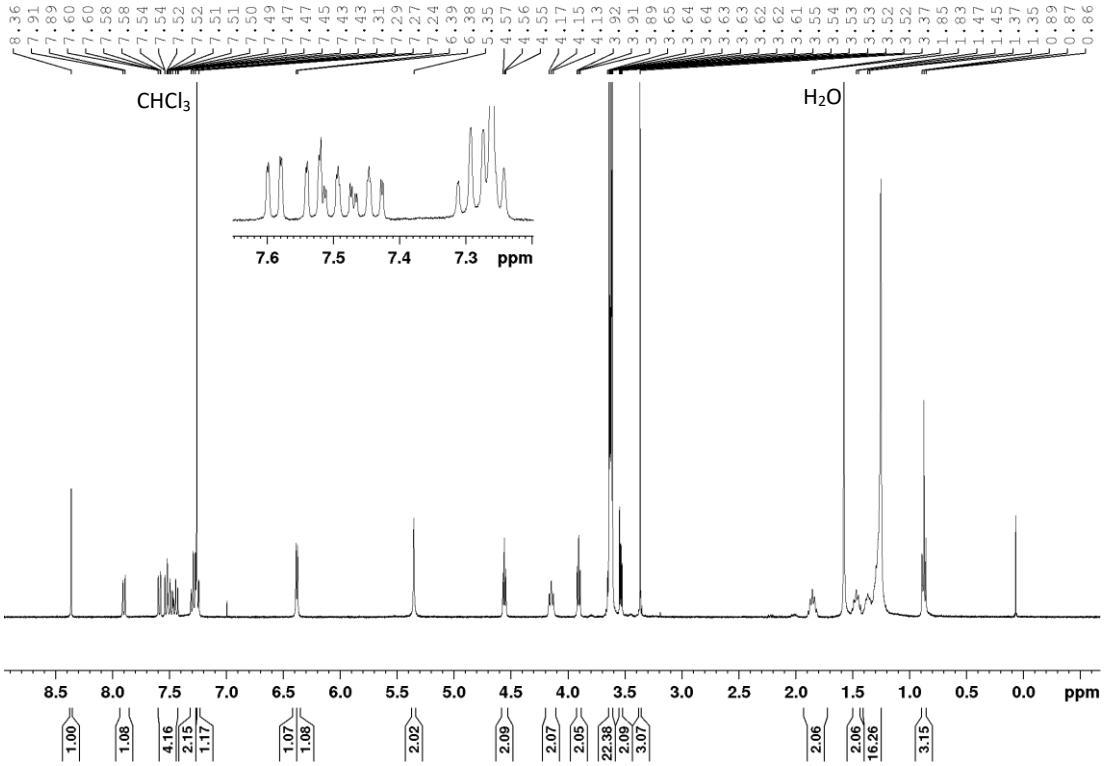

Figure S24. ^{1}H NMR (400 MHz, 295 K) spectrum of compound **SQ1** in $CDCl_3$.

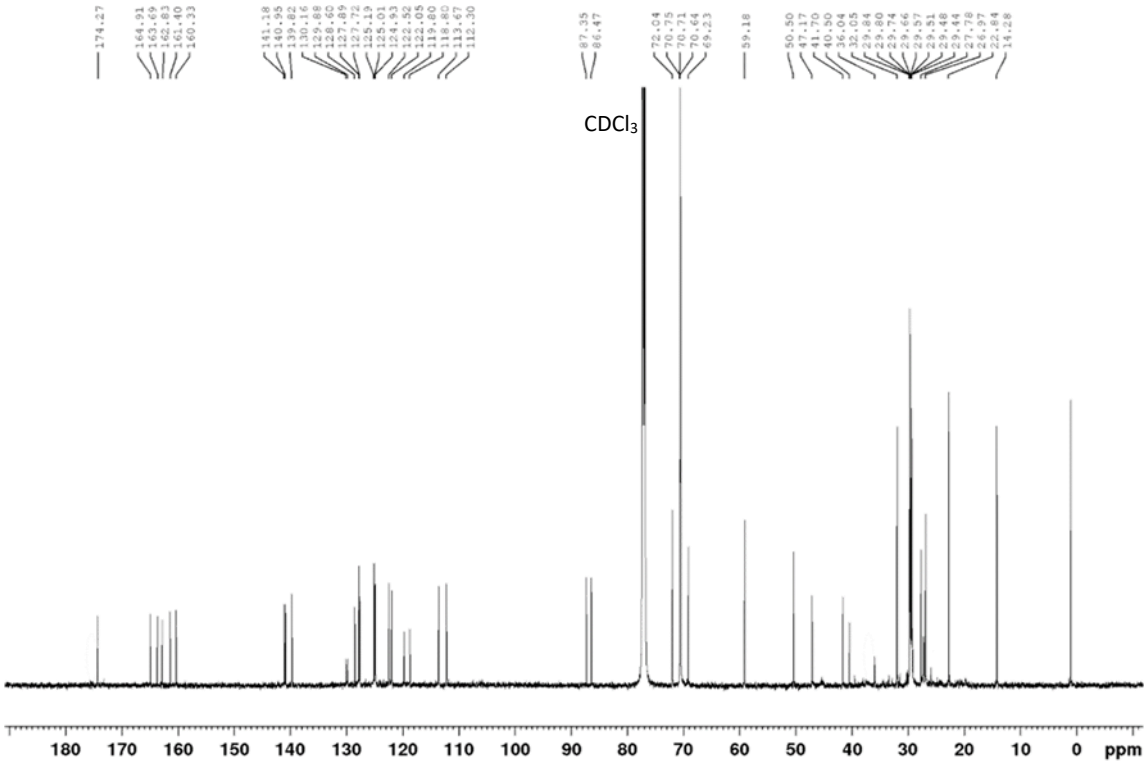

Figure S25. ^{13}C NMR (151 MHz, 295 K) spectrum of compound **SQ1** in $CDCl_3$.

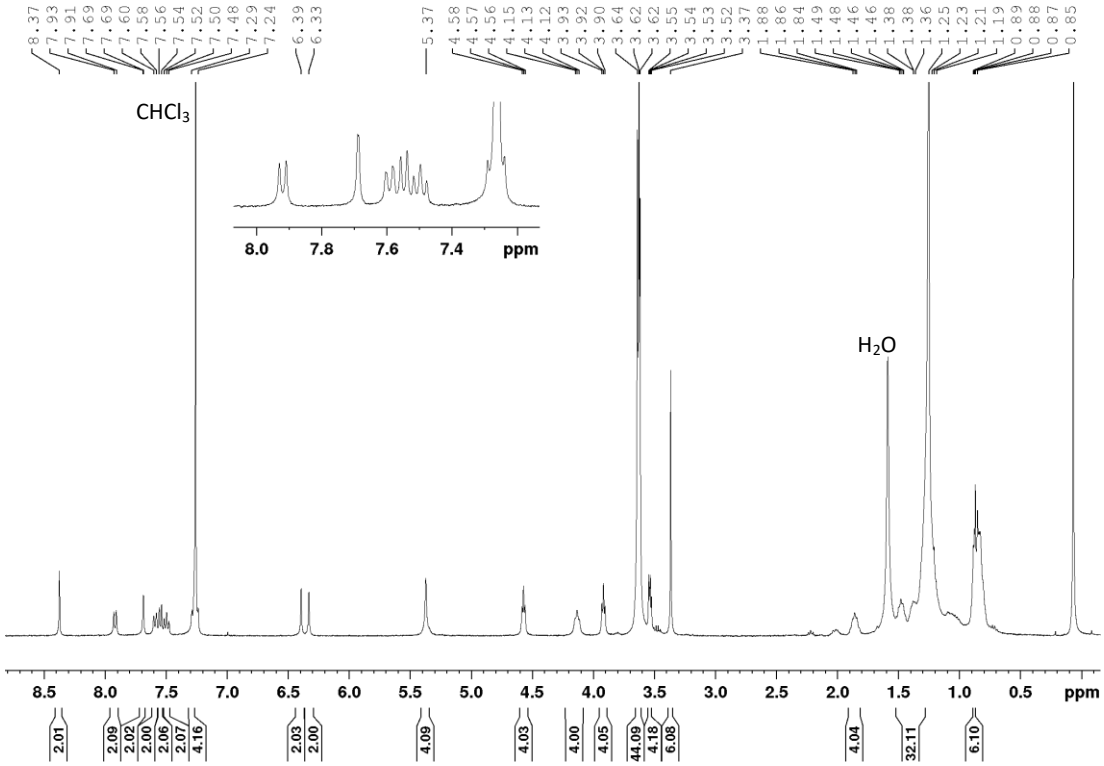

Figure S26. ^{1}H NMR (400 MHz, 295 K) spectrum of compound **BisSQ1** in $CDCl_3$.

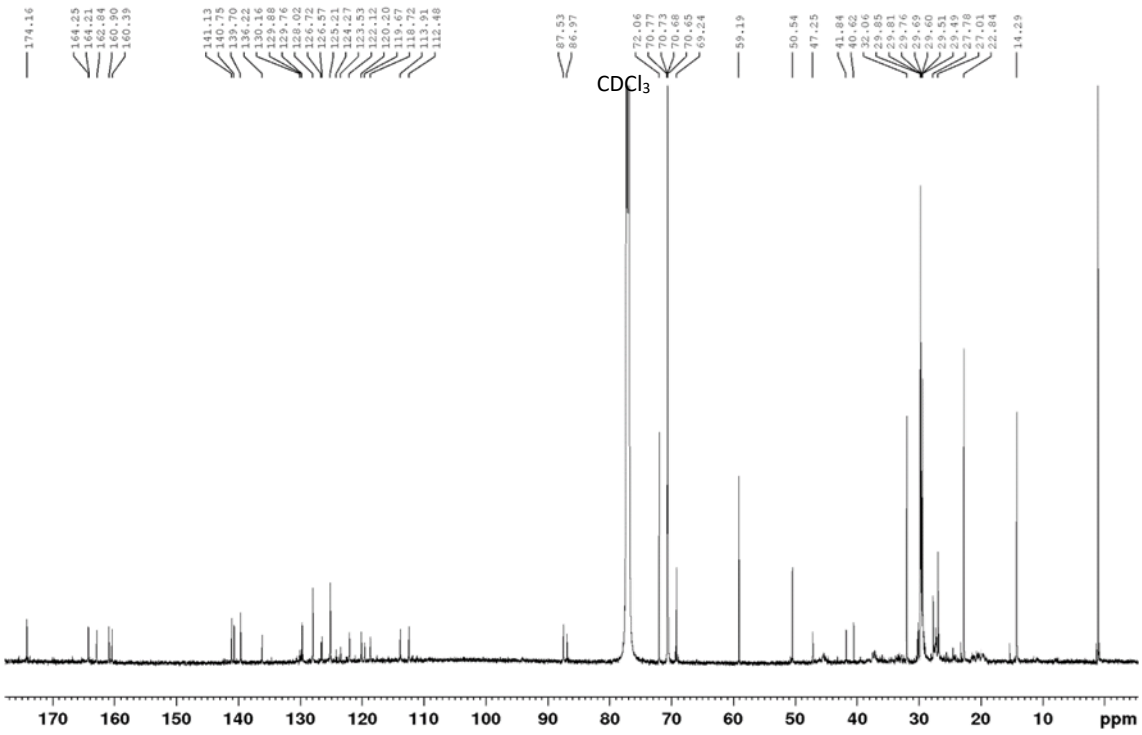

Figure S27. ^{13}C NMR (151 MHz, 295 K) spectrum of compound **BisSQ1** in $CDCl_3$.

9. References

S1 A. D. Becke, *J. Chem. Phys.* 1993, **98**, 5648−5652.

S2 C. Lee, W. Yang, R. G. Parr, Phys. Rev. B, 1988, **37**, 785−789.

S3 G. A. Petersson, A. Bennett, T. G. Tensfeldt, M. A. Al-Laham, W. A. Shirley, *J. Chem. Phys.*, 1988, **89**, 2193−2218.

S4 Gaussian 09, Revision D.01, M. J. Frisch, G. W. Trucks, H. B. Schlegel, G. E. Scuseria, M. A. Robb, J. R. Cheeseman, G. Scalmani, V. Barone, G. A. Petersson, H. Nakatsuji, X. Li, M. Caricato, A. Marenich, J. Bloino, B. G. Janesko, R. Gomperts, B. Mennucci, H. P. Hratchian, J. V. Ortiz, A. F. Izmaylov, J. L. Sonnenberg, D. Williams-Young, F. Ding, F. Lipparini, F. Egidi, J. Goings, B. Peng, A. Petrone, T. Henderson, D. Ranasinghe, V. G. Zakrzewski, J. Gao, N. Rega, G. Zheng, W. Liang, M. Hada, M. Ehara, K. Toyota, R. Fukuda, J. Hasegawa, M. Ishida, T. Nakajima, Y. Honda, O. Kitao, H. Nakai, T. Vreven, K. Throssell, J. A. Montgomery, Jr., J. E. Peralta, F. Ogliaro, M. Bearpark, J. J. Heyd, E. Brothers, K. N. Kudin, V. N. Staroverov, T. Keith, R. Kobayashi, J. Normand, K. Raghavachari, A. Rendell, J. C. Burant, S. S. Iyengar, J. Tomasi, M. Cossi, J. M. Millam, M. Klene, C. Adamo, R. Cammi, J. W. Ochterski, R. L. Martin, K. Morokuma, O. Farkas, J. B. Foresman, and D. J. Fox, Gaussian, Inc., Wallingford CT, 2016.

S5 T.-S. Ahn, R. O. Al-Kaysi, A. M. Müller, K. M. Wentz and C. J. Bardeen, *Rev. Sci. Instrum.*, 2007, **78**, 086105.

S6 M. M. J. Smulders, A. P. H. J. Schenning and E. W. Meijer, *J. Am. Chem. Soc.*, 2008, **130**, 606−611.

S7 M. M. J. Smulders, M. M. L. Nieuwenhuizen, T. F. A. de Greef, P. van der Schoot, A. P. H. J. Schenning and E. W. Meijer, *Chem. Eur. J.*, 2010, **16**, 362−367.

S8 F. Würthner, S. Yao, T. Debaerdemaeker and R. Wortmann, *J. Am. Chem. Soc.*, 2002, **124**, 9431−9447.

S9 R. B. Martin, *Chem. Rev.*, 1996, **96**, 3043−3064.

S10 T. E. Kaiser, V. Stepanenko and F. Würthner, *J. Am. Chem. Soc.*, 2009, **131**, 6719−6732.